Applied Acoustics 121 (2017) 74–81

Contents lists available at ScienceDirect

Applied Acoustics

journal homepage: www.elsevier.com/locate/apacoust

Meteorological effects on the noise reducing performance of a low parallel wall structure

Timothy Van Renterghem [a,*], Shahram Taherzadeh [b], Maarten Hornikx [c], Keith Attenborough [b]

[a] Ghent University, Department of Information Technology, Technologiepark 15, B-9052 Gent, Belgium
[b] The Open University, Department of Engineering and Innovation, Walton Hall, Milton Keynes MK7 6AA, UK
[c] Eindhoven University of Technology, Building Physics and Services, P.O. Box 513, 5600 MB, 17 Eindhoven, The Netherlands

ARTICLE INFO

Article history:
Received 24 October 2016
Received in revised form 11 January 2017
Accepted 26 January 2017

Keywords:
Outdoor sound propagation
Low parallel walls
Turbulence
Refraction of sound
Road traffic noise
Ground effects

ABSTRACT

Numerical calculations, scale model experiments and real-life implementations have shown that the insertion of a closely spaced array of low parallel walls of finite dimension beside a road is potentially useful for road traffic noise abatement. However, previous studies did not consider atmospheric effects. In this work, numerical techniques have been used to predict the sound reduction provided by a low parallel wall structure, subject to wind and temperature related atmospheric effects. Three full-wave prediction schemes show very good agreement when looking at the insertion loss of a low 6 m wide parallel wall structure, consisting of 24 regularly spaced 0.2-m high rigid walls. Meteorological effects are predicted not to deteriorate the insertion loss (relative to rigid flat ground) of the parallel wall array in the low frequency range. However, at high sound frequencies the insertion loss is strongly reduced by downward refraction at a distance of 50 m in case of strong wind. Consequently, overall A-weighted road traffic noise insertion loss will be significantly lower during wind episodes. Although weak turbulence does not alter the energy time-averaged insertion losses, strong turbulence reduces the noise shielding in the high frequency range also. As with conventional noise walls, when considering use of low parallel wall structures for noise reduction outdoors, even at short distances, atmospheric effects should be considered.

1. Introduction

Road traffic noise abatement by low parallel walls (LPWs), also called "parallel grooves" or "comblike" or "riblike" structures, can be tracked back to 1982 [1] (when only considering peer-reviewed journal papers). More recently, there has been a renewed interest in LPWs [2–5]. The advantages of such structures for noise abatement are the preservation of the openness of the landscape near the road (in strong contrast to the traditional noise wall), the fact that paths can be made through them without compromising their acoustic performance and their potentially low cost.

Bougdah et al. [2] discussed possible phenomena when sound waves interact with a LPW structure. The cavities formed by the parallel walls could act as quarter-wave length resonators; sound waves passing over the tops of the walls are partly cancelled at specific sound frequencies by reflections coming from the bottoms of the cavities. When regularly spaced, the parallel wall structure can also be seen as a diffraction grating, leading to distinct zones with constructive and destructive interference depending on the angle of incidence and receiver angle. Thirdly, the diffracted waves at the wall edges and the (delayed) reflected sound waves in between the cavities may interfere. Multiple paths are possible inside the grooves, leading to complex interference effects extending over relatively large frequency intervals. Given that all these effects occur simultaneously, their relative importance with respect to noise reduction is difficult to establish. In addition, especially for rolling noise being generated at only a few centimeters above the road surface, diffraction at the (effective) impedance discontinuity occurs, further complicating physical explanation. In Ref. [6], the effects observed with such LPW structures are called diffraction-assisted ground effects.

An important aspect of the acoustical performance of LPWs is that surface waves [7–9] will be excited resulting in a redistribution of spectral energy in sound propagating over them. In contrast to the aforementioned effects, surface waves lead to amplification of sound in a narrow band of frequencies. Sound energy is trapped in a zone close to the surface [8], and the decay of sound intensity with distance becomes less pronounced [8]. Conditions for surface wave generation are met when, upon grazing incidence,

* Corresponding author.
E-mail address: timothy.vanrenterghem@ugent.be (T. Van Renterghem).

http://dx.doi.org/10.1016/j.apacoust.2017.01.029
0003-682X/

the imaginary part of the equivalent surface impedance, by which such a LPW could be represented, exceeds its real part [1,2,10,8]. However, the surface waves can be mitigated by making the walls (partly) absorbing or by (partially) filling the space in between the walls with a porous medium such as gravel [3,9]. By doing so, a resistive part is added to the LPW's equivalent impedance which otherwise can be considered as purely reactive [7,1,2,9]. Other ways of reducing surface waves generated by LPWs are using a smaller number of walls [2] and introducing some randomness in the LPW structure [6].

The usefulness of parallel walls has been shown before by means of scale model studies [2,9,3], real-life implementations with artificial sound sources [1,3] and drive-by tests [3,5], and by numerical simulations [9,3]. So far, only the efficiency in a still and homogeneous atmosphere has been investigated.

Turbulence is known to strongly limit the magnitude of destructive interference dips that appear between direct sound and ground reflected sound outdoors [11,12]. Downward refraction of sound will lead to multiple sound paths arriving at a single receiver [11], and to changes in path length. Meteorological effects can be expected to affect the performance of LPWs at higher frequencies since LPWs are mainly related to interferences.

The main goal of this paper is to show the effect of refraction and turbulent scattering on the insertion loss of LPW structures by means of numerical predictions. Various techniques have been employed and the agreement between them might serve as a cross-validation of the predictions. A single (raised) LPW structure has been chosen for road traffic noise applications. Alternatively, sunken geometries [5,3] could have the benefit of allowing cars to drive over it when needed, meaning that a placement close to the traffic lanes (e.g. on the emergency lane or central reservation) is possible. However, such geometries perform slightly worse than the equivalent raised ones [3] in a non-refracting and non-turbulent atmosphere. The focus in this study is therefore on the latter.

This paper does not intend to provide a full parameter study of all parameters involved in LPWs, or simulating its performance in multi-lane road traffic noise cases. Such studies can be found elsewhere, see e.g. Refs. [9,3]. For simplicity, all surfaces are modelled as rigid, notwithstanding that this is known to promote surface waves. The interaction between atmospheric effects and individual LPW parameters like height, spacing, wall thickness etc. is not studied either.

2. Low parallel wall case

A source is positioned at (x, z) (0, 0.01) m, representative for the rolling noise source in road traffic [13,14], which is the dominant contribution in the direct vicinity of highways. Receivers are located at 50 m from the source, at heights of either 1.5 m (representing the average ear height of pedestrians) or 4 m (height of the first storey of buildings as commonly used in noise maps). All surfaces are rigid.

A regularly spaced LPW configuration was considered (see Figs. 1 and 2), containing 24 walls, all 0.2 m high and 0.065 m thick, starting at 2.5 m (i.e. the left face of the first wall) from the source, with a centre-to-centre spacing of 0.26 m. The right face of the last wall is positioned at 8.545 m from the source. The dimensions of the LPWs considered here are roughly based on household bricks placed on their sides; using such bricks could be a cheap way of constructing a LPW in practice. A minimum distance between the first wall and the source is needed for safety reasons.

3. Numerical techniques and parameters

3.1. Sound propagation models

Three numerical techniques have been used to assess the sound pressure level reduction provided by the LPWs, which are shortly described in the subsequent subsections. Discriminating features of the numerical techniques are the possibility to model wind and/or turbulence, whether calculations were performed in two dimensions or in 3D, and whether the effective sound speed approach [11,15] was used or the (full) Linearised Euler Equations (LEE) [16–18] were solved when modelling wind effects. The frequency range considered contains the 1/3 octave bands between 50 Hz and 2500 Hz.

3.1.1. BEM

The boundary element method (BEM) is a well-established technique solving the Helmholtz equation in the frequency domain. Simulations are here limited to sound propagation in a still and homogeneous atmosphere. Calculations were performed in 2D with explicitly modelled parallel walls using the code described in Ref. [6]. The method used 10 computational cells per wavelength and allows for exactly positioning discretisation points at the wall-air interfaces. Reflection from the underlying ground is included in the Green's function and therefore the ground was not discretised. This greatly reduces the computational effort. Six frequencies were calculated to constitute each 1/3 octave band.

3.1.2. FDTD

The pressure-velocity (P-V) staggered-in-place (SIP) staggered-in-time (SIT) finite-difference time-domain (FDTD) model [19] is used. When relying on the effective sound speed approach, accurate results can be obtained in the case of wind flowing parallel to flat ground [20], while keeping the computational cost significantly smaller than fully solving the LEE (see also Appendix B).

The spatial discretisation step was chosen to be 1 cm, sufficiently small for resolving the 2.5-kHz 1/3 octave band. The temporal discretisation was set to 20 μs, ensuring numerical stability, optimal computing speed and minimum phase error [21]. On the left, right and upper boundaries, perfectly matched layers [22] are placed to simulate continuation of the propagation region and thus zero-reflection calculation domain termination. The PML equations use the effective sound speed approach as well, by taking the effective sound speeds appearing closest to the inner region of the simulation domain [19].

The parallel walls were explicitly modelled with best fitting square cells, which comes at no additional (numerical) cost given

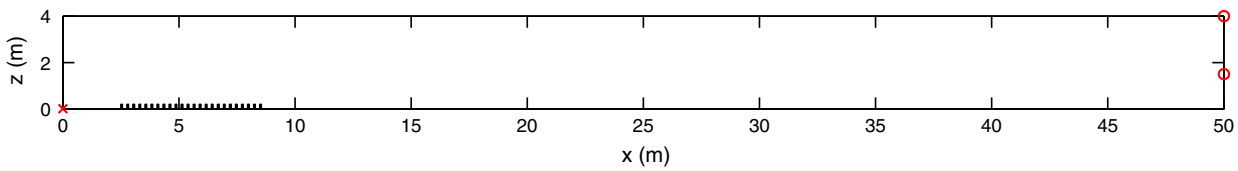

Fig. 1. Geometry studied, indicating the low parallel wall structure, the source (cross) and receivers (open circles).

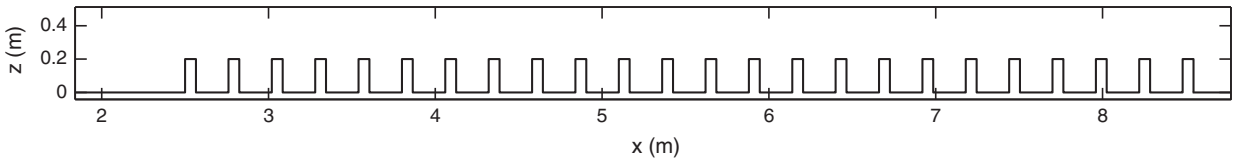

Fig. 2. Detail of the LPW structure.

this is a volume discretisation technique. A single simulation [19] was sufficient to calculate the full frequency range of interest.

3.1.3. PSTD

The pseudospectral time-domain (PSTD) method [23] is closely related to the FDTD technique. However, this numerical technique is more efficient (in case of rigid geometries) as only 2 computational cells per wavelength are needed for its spatial discretisation, while phase errors are only introduced by the time iteration scheme. As a result, this model allows 3D applications [24], meaning that sound propagating obliquely over the parallel walls could be studied with a reasonable amount of computing power. PSTD can use either the effective sound speed approach or full solution of the LEE to study the effect of wind refraction (see Appendix B). In case of 3D simulations, a finite domain in the transverse direction with periodic boundary conditions is applied (similar to the approach as described in Ref. [25]) and lattice configurations were modelled. The reader is referred to Appendix C for a comparison between 2D and 3D insertion losses. A spatial discretization step of 0.0325 m was chosen in PSTD to capture the geometry of the walls, and a PML approach similar to FDTD was used.

3.2. Atmospheric effects

Refraction by wind and turbulent scattering is of main interest in current work. A reference sound speed of 340 m/s is considered and the air's mass density is set to 1.2 kg/m^3. Atmospheric absorption is not considered given the main focus on insertion losses for which this effect would cancel out to a large extent.

3.2.1. Wind

In this work, refraction by a logarithmic wind speed profile is modelled, representative for a neutral atmosphere:

$$u_z = \frac{u_*}{\kappa} \ln\left(\frac{z}{z_0}\right),$$

with u_z the wind speed at height z, u_* the friction velocity, and κ the von Kármán constant (=0.4). The wind speed is assumed to be directed parallel to the surface. Friction velocities of $u_* = 0.4$ m/s and 0.8 m/s have been used, and will be further indicated as moderate and strong wind, respectively. Exact downwind sound propagation was assumed with the wind component orthogonal to the length axes of the parallel walls. A roughness length z_0 of 1 cm is taken, representative for open flat terrain in absence of obstacles. The effect of the parallel walls on the wind flow is not accounted for and would need detailed computational fluid dynamics (CFD) simulations. To account for the additional surface roughness induced by the LPW structure, an additional simulation with an increase in z_0 has been modelled in Appendix A.

3.2.2. Turbulence

Scattering by a turbulent atmosphere is simulated with FDTD using the turbule theory proposed in Refs. [26,27]. The turbule approach is highly suitable in a full-volume discretisation technique like FDTD [19]. The (otherwise uniform) temperature in the sound propagation domain is perturbed, resulting in local variations in the sound speed (see Fig. 3). Many of such turbulent realisations were generated and sound propagation through each "frozen turbulence" field was explicitly calculated. The realisations were constructed in a such a way that their energy and spectral statistics correspond to experimental observations. Cases were modelled by assuming weak (structure factor $C_T^2 = 0.05$ K^2/m$^{2/3}$) or strong temperature related atmospheric turbulence ($C_T^2 = 2$ K^2/m$^{2/3}$) in absence of wind. The strong structure factor falls within the range of measured values outdoors near a large obstacle [28]. Given the fact that LPWs might appear close to moving vehicles, the air displacement by cars could generate a large amount of turbulence. Although a more detailed assessment of this particular effect is beyond the scope of the current work, the rather large degree of turbulence used here could be considered to mimic such effects. The smaller value corresponds to the range of values reported in Ref. [15] near (flat) ground during a summer's day.

The turbule model simulates a homogeneous and isotropic turbulent atmosphere following a Kolmogorov spectral density function, with an exponential decay from the perturbed temperature maximum at the turbule centre towards its surroundings [27]. The Kolmogorov turbulence spectrum can be considered as a universally applicable and realistic representation of the atmosphere

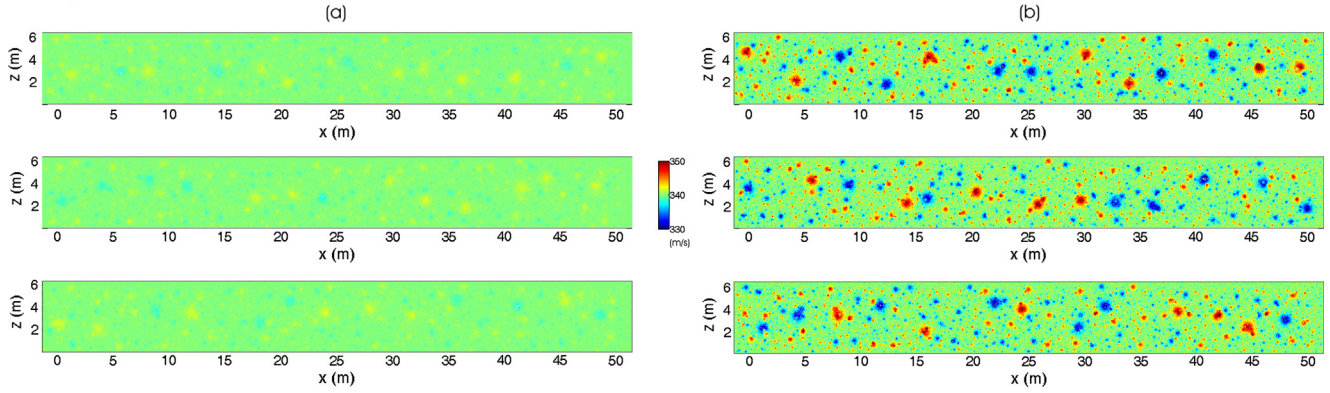

Fig. 3. Spatial sound speed distribution in case of (a) weak ($C_T^2 = 0.05$ K^2/m$^{2/3}$) and (b) strong ($C_T^2 = 2$ K^2/m$^{2/3}$) temperature turbulence. Three realisations are depicted for each turbulence strength. In absence of turbulence, a uniform field with a sound speed of 340 m/s was modelled.

in the inertial subrange [15]. Eight length scales are considered, ranging from 1.5 cm to 2 m, fitting in between the grid resolution and the extent of the simulation domain. Other turbule-model parameters are the packing fraction $\phi = 0.002$, $\mu = \ln(2)$ and a ratio of "cell" size to turbule size d/a = 8. The reader is referred to Ref. [27] for more details on these parameters and related equations.

To purely see the effect of turbulent scattering on sound shielding, sound propagation is simulated in a non-moving atmosphere. New realisations were added until the energetically averaged insertion losses converged; the convergence criterion was a change in insertion loss of less than 0.1 dB at all one-third octave bands considered. For the weak turbulence case, 15 calculations sufficed. For the strong turbulent case, 40 realisations have been calculated.

4. Numerical predictions

The insertion loss (IL) is calculated as the sound pressure level in case of flat rigid ground (i.e. reference case) minus the sound pressure level in presence of the LPWs for an identical source-receiver setup. Positive values mean that sound pressure levels are reduced. For the LPW scenarios with wind and turbulence, exactly the same wind profiles and turbulent fields have been considered in the reference case.

4.1. Still and homogeneous atmosphere

The insertion loss spectrum of the LPW structure (see Fig. 4) shows a pronounced frequency-dependent behavior. At very low frequencies, the small walls are negligible relative to the large wavelengths and a similar sound propagation situation as above flat rigid ground is obtained. The surface waves that are excited by the LPWs yield a negative insertion loss, meaning that an increase in sound pressure level is predicted over and above that due to the constructive interference (amounting to +6 dB relative to free field sound propagation) predicted for the reference situation. Surface waves are most pronounced between 100 and 200 Hz. At higher frequencies, strong positive insertion losses are calculated, exceeding 10 dB in some frequency ranges. The higher receiver position gives rise to a somewhat lower insertion loss, especially at the highest sound frequencies considered.

The agreement between the full-wave techniques BEM, FDTD and PSTD is excellent. Some small differences are inevitable, since the methods that were used are quite diverse: a frequency-domain technique is opposed to time-domain approaches, and the methods use very different spatial (and temporal) resolutions. In addition, the time-domain techniques use – implicitly – a large number of sound frequencies to constitute the 1/3 octave bands

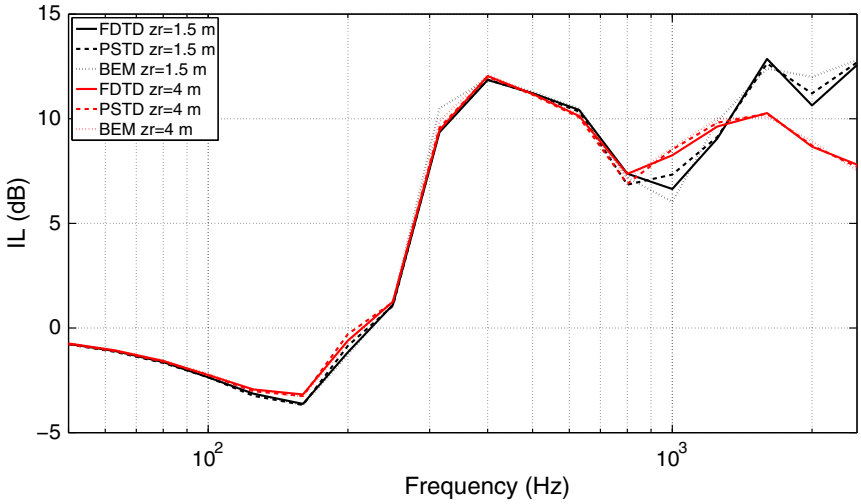

Fig. 4. Insertion loss spectra in case of a windless atmosphere. 2D predictions were performed with FDTD, BEM and PSTD explicitly modelling the LPW structure, for a receiver height z_r of 1.5 m and 4 m.

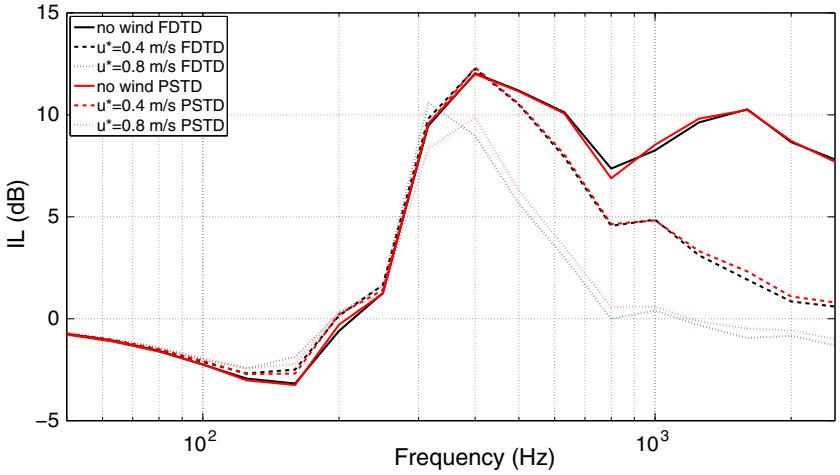

Fig. 5. Insertion loss spectra in case of a windless atmosphere, and in presence of moderate ($u^* = 0.4$ m/s) and strong ($u^* = 0.8$ m/s) wind. Predictions were performed with FDTD and PSTD for a receiver height of 4 m. In all predictions, the effective sound speed approach was used and calculations are two-dimensional.

by relying on the response of an acoustic pulse as source excitation [19]. With the BEM technique, a new simulation has to be initiated for each frequency of interest.

4.2. Wind

Fig. 5 shows the results for the scenarios with wind. The low frequency range up to 250 Hz, including the surface wave zone, is not affected by the presence of wind; this is consistent with the fact that low frequencies are typically less sensitive to atmospheric refraction [11]. With increasing wind speed, the insertion loss predicted in a still atmosphere is partly lost above 300–400 Hz. In case of strong wind, zero insertion loss is predicted starting from about 1 kHz. However, the steep increase in IL between 200 and 300 Hz, going from 0 to 10 dB, is not affected by the wind.

The agreement between the FDTD and PSTD technique is again very good. With standard BEM, predictions including the effect of wind are not possible.

The effect of accounting for the (small) increase in aerodynamic roughness length by the presence of the LPW hardly influences the noise shielding (see Appendix A). The use of the effective sound speed approach (see Appendix B), and modelling a coherent line source in front of a LPW to represent a 3D lattice combined with an incoherent line source (see Appendix C), both in order to alleviate the computational cost, show to be good assumptions for this specific LPW structure and the source-receiver geometry considered.

4.3. Turbulence

The effect of temperature related turbulence on the LPW's insertion loss is presented in Fig. 6. The effect of turbulent scattering by atmospheric inhomogeneities is very small at low sound frequencies, and becomes pronounced at higher frequencies. For the weakly turbulent case, the average insertion loss is very close to the no turbulence case. In case of strong turbulence, there will be a general loss in insertion loss starting from about 400 Hz, although some frequencies might be positively affected even at the time-averaged response (significant at 315 Hz). Strong turbulence causes large variations in between the various turbulent realisations that have been modelled with FDTD, illustrated by the magnitude of the error bars in Fig. 6.

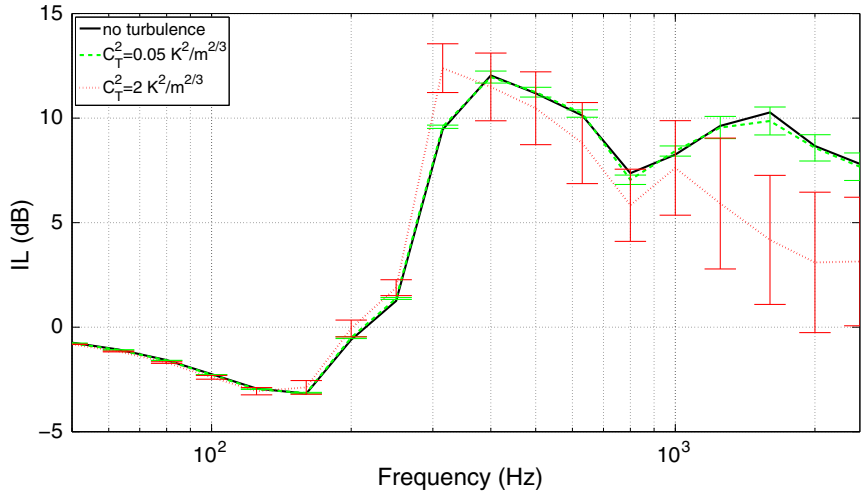

Fig. 6. Insertion loss spectra in absence of turbulence, and in case of weak (C_T^2 = 0.05 K^2/m$^{2/3}$) and strong (C_T^2 = 0.05 K^2/m$^{2/3}$) temperature related turbulence. The error bars have a total length of two times the standard deviations based on the individual realisations. Predictions were performed with 2D FDTD for a receiver height of 4 m in absence of wind.

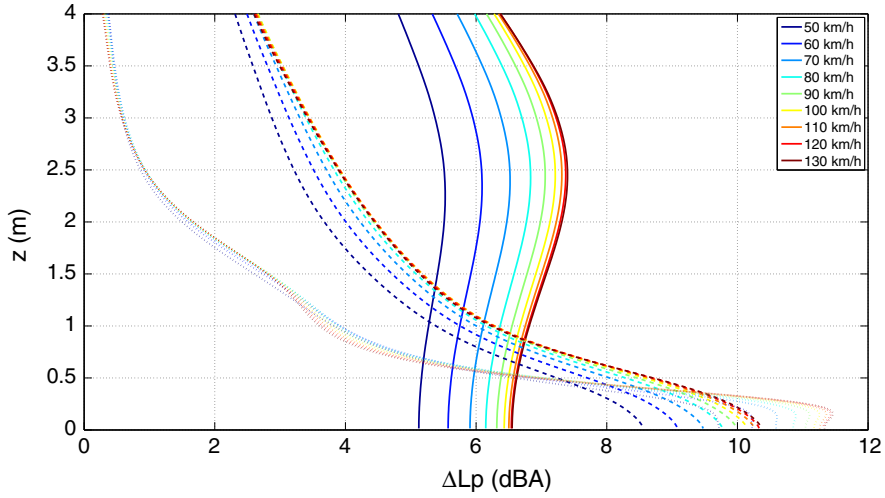

Fig. 7. Total A-weighted road traffic noise insertion loss for the LPW structure as a function of receiver height, for a range of vehicle speeds in absence of wind (full lines), in moderate wind (dashed lines, u* = 0.4 m/s) and in strong wind (dotted lines, u* = 0.8 m/s). 15% heavy traffic has been assumed. The LPW responses were calculated with 2D FDTD, at a receiver at 50 m from the traffic lane.

5. Road traffic noise

Given that the insertion loss of the LPW is strongly frequency dependent, and given that also the road traffic source power spectrum strongly depends on sound frequency, it is of practical use to combine both to estimate its total A-weighted road traffic noise insertion loss. The Harmonoise/Imagine road traffic source power spectrum [14], providing data in 1/3 octave bands, was used.

Given the good agreement between the full-wave numerical techniques, the FDTD results were used for these calculations (see Fig. 7). In accordance with the Harmonoise/Imagine road traffic source power model, emissions from 3 source heights (namely 1 cm, 30 cm and 75 cm) have been calculated. A receiver distance of 50 m is used, similar to the aforementioned simulations. The percentage of heavy traffic was set at 15%. Vehicles speeds, ranging from 50 km/h to 130 km/h, in steps of 10 km/h, were taken. The traffic noise situation involved a single traffic lane only.

The predictions show that at a receiver height of 1.5 m and 50 m range, the road traffic noise insertion loss ranges roughly between 5 and 7 dBA in absence of wind. At lower vehicle speeds, insertion losses are more modest due to the larger importance of low frequencies that are less attenuated or even amplified by the LPW structure. In case of higher driving speeds, the maximum in source spectrum shifts towards higher frequencies where the LPW performs better. For the moderate and strong wind, the influence of vehicle speed is less pronounced, and a significantly lower shielding is predicted at heights of practical relevance. However, close to the ground, a strong reduction in road traffic sound pressure levels is predicted. While for the moderate wind about 4–5 dBA is left at 1.5 m, the road traffic noise insertion loss becomes near 3 dBA for the strong wind. At higher positions, the effect of wind becomes much more pronounced.

6. Conclusions

In this purely numerical study, a specific raised low parallel wall structure (consisting of 20 cm high rigid walls, regularly and closely spaced, with a total width of 6 m) has been analysed at short range. Focus is on the performance of such a road traffic noise reducing measure at 50 m in realistic atmospheres outdoors. In case of a rigid LPW structure placed above rigid ground, amplification of sound by surface waves in the low frequency range is observed, acting more or less independent of atmospheric effects. Complex interference effects yield useful sound reduction at medium and high sound frequencies in a still atmosphere. This frequency range is, however, highly sensitive to the action of (down)wind, leading to multiple sound paths arriving at a receiver and pronounced phase changes, negatively affecting their noise reduction potential. The strong wind modelled in this work leads to zero insertion loss above the 1 kHz 1/3 octave band. When applied to a road traffic noise spectrum, this leads to a total A-weighted insertion loss close to 0, independent of the vehicle speed, at a receiver height of 4 m. At lower receiver heights more of the insertion loss predicted in a windless atmosphere is retained (still 3 dBA at 1.5 m high). The presence of temperature related atmospheric turbulence negatively effects the energetically averaged insertion loss of the LPW structure, but only for high sound frequencies and in case of strong turbulence.

Three different full-wave numerical calculation schemes (BEM, FDTD and PSTD), explicitly resolving for the rigid LPWs in their computational domains, agree very well in case of a still atmosphere over the full frequency range of interest. In case of a windy atmosphere, calculations with FDTD and PSTD coincide nicely. These agreements might serve as a cross-validation of the numerical results obtained.

Acknowledgements

The current work was initiated during the HOSANNA project (European Community's Seventh Framework Programme, under Grant agreement No. 234306), whose financial report was gratefully acknowledged.

Appendix A. Aerodynamic roughness length

The main effect of the low walls on the wind flow is most likely an increase in the aerodynamic roughness length z_0, at least in a part of the simulation domain. A rough estimate yields a value of 3 cm (when taking additionally one tenth of the LPW heights [29]). The comparison between spectral insertion loss in case of a roughness length of 1 cm and 3 cm, imposed over the full computational domain, as depicted in Fig. A1, for both moderate and strong wind, shows only small differences. This holds for both the receiver height of 1.5 m (not shown) and 4 m.

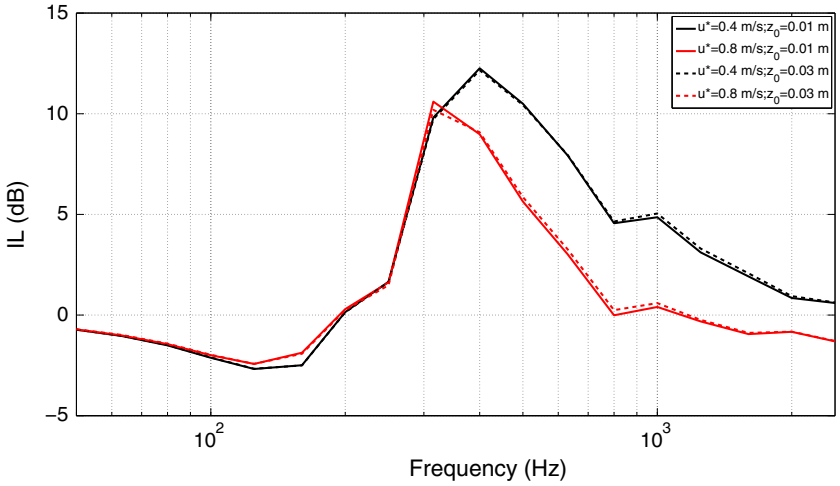

Fig. A1. Insertion loss spectra in case of a moderate (u^* = 0.4 m/s) and strong (u^* =0.8 m/s) wind, for two values of the aerodynamic roughness length z_0 (imposed over the full computational domain). Predictions were performed with FDTD, for a receiver height of 4 m. The effective sound speed approach was used and calculations are two-dimensional.

Appendix B. Effective sound speed approach

For the simulations in this work, a range-independent wind speed profile is assumed, parallel to the ground surface. The conditions for applying the effective sound speed approach are thus met. The PSTD calculations shown in Fig. B1 confirm that the effective sound speed approach is a reasonably accurate alternative to fully solving the LEE equations (receiver height of 4 m). The insertion loss spectrum at the 1.5-m high receiver shows very similar differences between these approaches. The main advantage is a strong decrease in computing times and memory demands.

Appendix C. Incoherent line source and lattice structure

The 2D simulations performed in this work imply that a coherent line source is modelled. However, road traffic noise is better represented by an incoherent line source. A comparison between the coherent line source insertion loss and the one from an incoherent line source is shown in Fig. C1. For the latter, 3D PSTD has been used to calculate point source responses for paths where sound propagates obliquely over the LPW structure. For a given array width and height, lattice arrangements (by adding an identical LPW structure rotated over 90°) give a superior performance for road traffic noise reduction [3,30] compared to LPWs (implicitly assumed by performing 2D simulations). Therefore, such a lattice arrangement was chosen for the 3D calculations and should be used in practice to avoid the reduced performance at oblique sound paths. In a next step, these responses where aggregated to an incoherent line source insertion loss.

Although some differences can be observed, the insertion loss spectrum is rather similar and justifies the use of two-dimensional simulations performed in this work, largely reducing the computational cost. The coherent line source LPW simulations are thus very similar to those from the incoherent line source lattices. In case of wind, both the 2D PSTD and 3D PSTD calculations here solve the LEE.

The PSTD calculations for this additional analysis use a larger spatial discretization of 0.065 m. Although this discretization should be sufficient to accurately compute the frequency range of interest, some small deviations can be found compared to the finer discretization of 0.0325 m as used elsewhere in this paper. These differences mainly come from more coarsely representing the corners of the walls.

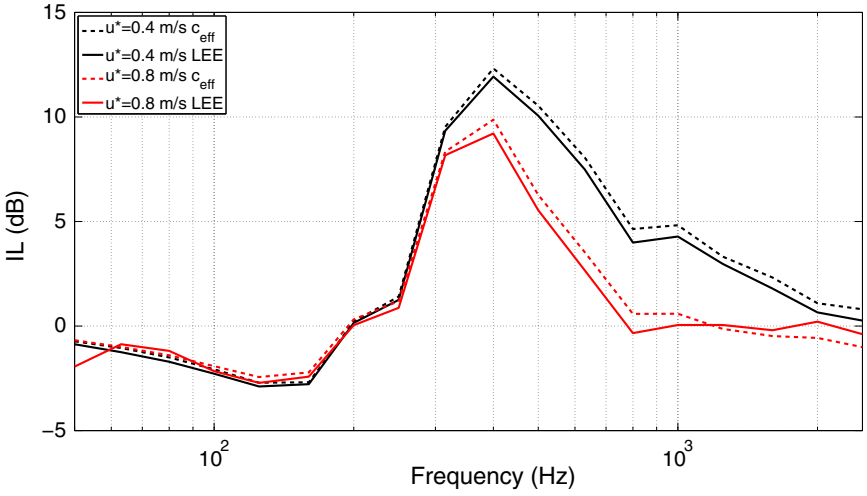

Fig. B1. Insertion loss spectra in case of a moderate ($u^* = 0.4$ m/s) and strong ($u^* = 0.8$ m/s) wind, using the effective sound speed approach (c_{eff}) and fully solving the Linearised Euler Equations (LEE). Predictions were performed with PSTD, for a receiver height of 4 m. Calculations are two-dimensional.

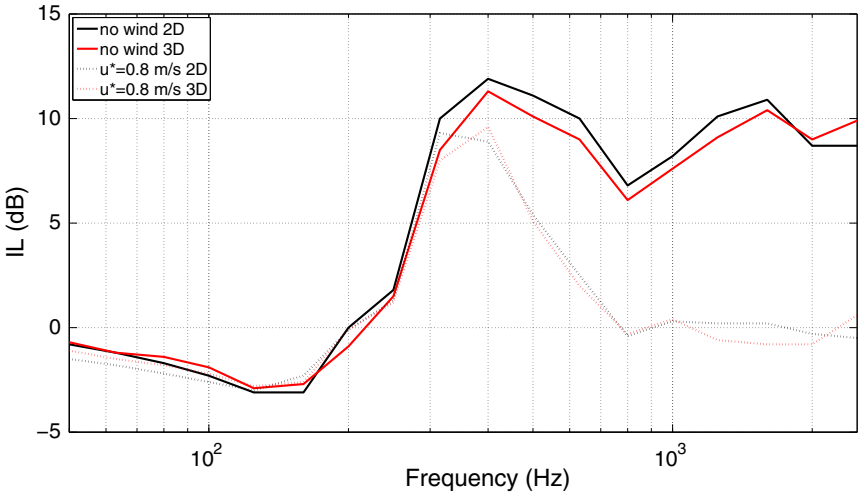

Fig. C1. Insertion loss spectra in a still atmosphere and strong ($u^* = 0.8$ m/s) wind, for a coherent (2D, LPW, LEE in case of wind) and incoherent line source (3D, lattice structure, LEE in case of wind). Predictions were performed with PSTD, for a receiver height of 4 m.

References

[1] van der Heijden L, Martens M. Traffic noise reduction by means of surface wave exclusion above parallel grooves in the roadside. Appl Acoust 1982;15:329–39.
[2] Bougdah H, Ekici I, Kang J. A laboratory investigation of noise reduction by rib-like structures on the ground. J Acoust Soc Am 2006;120:3714–22.
[3] Bashir I, Hill T, Taherzadeh S, Attenborough K, Hornikx M. Reduction of surface transport noise by ground roughness. Appl Acoust 2014;83:1–15.
[4] Van Renterghem T, Forssen J, Attenborough K, Jean P, Defrance J, Hornikx M, et al. Using natural means to reduce surface transport noise during propagation outdoors. Appl Acoust 2015;92:86–101.
[5] Hooghwerff J, Reinink F, Van Der Heijden R, Wijnant Y. Whisstone, a sound diffractor: does it really affect traffic noise? Proc Euronoise 2015:1297–302.
[6] Bashir I, Taherzadeh S, Attenborough K. Diffraction assisted rough ground effect: models and data. J Acoust Soc Am 2013;133:1281–92.
[7] Donato R. Model experiments on surface waves. J Acoust Soc Am 1978;63:700–3.
[8] Embleton T. Tutorial on sound propagation outdoors. J Acoust Soc Am 1996;100:31–48.
[9] Bashir I, Taherzadeh S, Attenborough K. Surface waves over periodically-spaced strips. J Acoust Soc Am 2013;134:4691–7.
[10] Attenborough K. Acoustical characteristics of porous materials. Phys Rep 1982;82:177–225.
[11] Salomons E. Computational atmospheric acoustics. Dodrecht: Kluwer; 2001.
[12] Attenborough K, Li K, Horoshenkov K. Predicting outdoor sound. London and New York: Taylor and Francis; 2007.
[13] Sandberg U, Ejsmont J. Tyre/road noise reference book. Kisa, Sweden: Informex; 2002.
[14] Jonasson H. Acoustical source modelling of road vehicles. Acta Acust United Acust 2007;93:173–84.
[15] Ostashev V, Wilson D. Acoustics in moving inhomogeneous media. 2nd ed. Boca Raton, USA: CRC Press; 2016.
[16] Blumrich R, Heimann D. A linearized Eulerian sound propagation model for studies of complex meteorological effects. J Acoust Soc Am 2002;112:446–55.
[17] Van Renterghem T, Botteldooren D. Numerical simulation of the effect of trees on downwind noise barrier performance. Acta Acust United Acust 2003;89:764–78.
[18] Ostashev V, Wilson D, Liu L, Aldridge D, Symons N, Marlin D. Equations for finite-difference, time-domain simulation of sound propagation in moving inhomogeneous media and numerical implementation. J Acoust Soc Am 2005;117:503–17.
[19] Van Renterghem T. Efficient outdoor sound propagation modelling with the finite-difference time-domain (FDTD) method: a review. Int J Aeroacoust 2014;13:385–404.
[20] Blumrich R, Heimann D. Numerical estimation of atmospheric approximation effects in outdoor sound propagation modelling. Act Acust United Acust 2004;90:24–37.
[21] Van Renterghem T, Botteldooren D. Prediction-step staggered-in-time FDTD: an efficient numerical scheme to solve the linearised equations of fluid dynamics in outdoor sound propagation. Appl Acoust 2007;68:201–16.
[22] Berenger J. A perfectly matched layer for the absorption of electromagnetic waves. J Comput Phys 1994;114:185–200.
[23] Hornikx M, Waxler R, Forssén J. The extended Fourier pseudospectral time-domain method for atmospheric sound propagation. J Acoust Soc Am 2010;128:1632–46.
[24] Hornikx M, Forssen J. Modelling of sound propagation to three-dimensional urban courtyards using the extended Fourier PSTD method. Appl Acoust 2011;72:665–76.
[25] Hornikx M, Van Renterghem T. Numerical investigation of the effect of crosswind on sound propagation outdoors. Act Acust United Acust 2016;102:558–67.
[26] Goedecke G, Auvermann H. Acoustic scattering by atmospheric turbules. J Acoust Soc Am 1997;102:759–71.
[27] Goedecke G, Wood R, Auvermann H, Ostashev V, Havelock D, Ting C. Spectral broadening of sound scattered by advecting atmospheric turbulence. J Acoust Soc Am 2001;109:1923–34.
[28] Forssén J, Ögren M. Thick barrier noise-reduction in the presence of atmospheric turbulence: measurements and numerical modelling. Appl Acoust 2002;63:173–87.
[29] Lettau H. Note on aerodynamic roughness-parameter estimation on the basis of roughness-element description. J Appl Meteorol 1969;8:828–32.
[30] Attenborough K, Bashir I, Taherzadeh S. Exploiting ground effects for surface transport noise abatement. Noise Map 2016;3:1–25.